An electrostatic potassium channel opener targeting the final voltage sensor transition

Sara I. Börjesson and Fredrik Elinder

Department of Clinical and Experimental Medicine, Division of Cell Biology, Linköping University, SE-581 85 Linköping, Sweden

Free polyunsaturated fatty acids (PUFAs) modulate the voltage dependence of voltage-gated ion channels. As an important consequence thereof, PUFAs can suppress epileptic seizures and cardiac arrhythmia. However, molecular details for the interaction between PUFA and ion channels are not well understood. In this study, we have localized the site of action for PUFAs on the voltage-gated Shaker K channel by introducing positive charges on the channel surface, which potentiated the PUFA effect. Furthermore, we found that PUFA mainly affects the final voltage sensor movement, which is closely linked to channel opening, and that specific charges at the extracellular end of the voltage sensor are critical for the PUFA effect. Because different voltage-gated K channels have different charge profiles, this implies channel-specific PUFA effects. The identified site and the pharmacological mechanism will potentially be very useful in future drug design of small-molecule compounds specifically targeting neuronal and cardiac excitability.

The Journal of General Physiology

INTRODUCTION

Polyunsaturated fatty acids (PUFAs) are components of phospholipids in the cell membrane, where they contribute to the fluidity and directly affect the activity of membrane proteins such as voltage-gated ion channels (Schmidt et al., 2006; Börjesson and Elinder, 2008; Y. Xu et al., 2008). In addition, free PUFAs play important physiological roles by affecting different membrane proteins, including ion channels (Boland and Drzewiecki, 2008; Sfondouris et al., 2008), and beneficial effects of PUFAs on heart arrhythmias and epilepsy have been reported (Lefevre and Aronson, 2000; Leaf et al., 2003). We suggested previously that PUFAs are important active substances in the fat-rich ketogenic diet used to treat severe epilepsy, by acting on voltage-gated K (Kv) channels (X.P. Xu et al., 2008). Specifically, PUFAs shift the voltage dependence of activation of the Shaker Kv channel via an electrostatic mechanism (Börjesson et al., 2008, 2010) (schematized in Fig. 1, A and B). Small shifts can have surprisingly large effects on excitability; a −5-mV shift is equivalent to increasing the number of K channels by a factor of 3 in the frog myelinated axon (Börjesson et al., 2010). The charge of the PUFA head group determines the direction of the effect, which has been referred to as the lipoelectric mechanism (Börjesson et al., 2008, 2010). However, because the site of action of PUFA on voltage-gated ion channels is unknown, the actual molecular mechanism of action for PUFA was hitherto unclear.

PUFAs partition into the cell membrane and likely interact with the channel at several positions, but the most likely target for the lipoelectric effect is the voltage sensor itself. In this study, we first set out to identify the site of action for PUFAs on Kv channels (referred to as the "PUFA action site" throughout). This is of crucial importance for understanding the mechanism by which PUFAs affect voltage-gated ion channels and for understanding why different channels are differently sensitive to PUFAs. A centrally located ion-conducting pore domain of the voltage-gated ion channel is surrounded by four voltage sensor domains (VSDs; Fig. 1 C) (Long et al., 2007; Börjesson and Elinder, 2008). Each VSD is composed of four transmembrane segments (S1–S4) (Long et al., 2007). S4 contains 4–10 positively charged residues responding to changes in the membrane voltage by sliding along negative charges in S1–S3, thereby turning the channel on or off (Tombola et al., 2006; Börjesson and Elinder, 2008). Several pharmacologically important sites have been identified in voltage-gated ion channels (Catterall et al., 2007; Börjesson and Elinder, 2008) (Fig. 1 C). These include: (a) Pore-blocking compounds (α-KTx for K channels), such as the scorpion charybdotoxin and agitoxins, which bind to the extracellular entrance of the ion-conducting pore; (b) quaternary ammonium compounds, such as local anaesthetics,

Correspondence to Fredrik Elinder: fredrik.elinder@liu.se

Abbreviations used in this paper: DHA, 4,7,10,13,16,19-all-cis-docosahexaenoic acid; $MTSEA^+$, 2-aminoethyl methanethiosulfonate hydrochloride; $MTSES^-$, sodium [2-sulfonatoethyl] methanethiosulfonate; $MTSET^+$, [2-(trimethylammonium)ethyl] methanethiosulfonate bromide; PUFA, polyunsaturated fatty acid; VSD, voltage sensor domain.

The Rockefeller University Press $30.00
J. Gen. Physiol. Vol. 137 No. 6 563–577
www.jgp.org/cgi/doi/10.1085/jgp.201110599

antiarrhythmics, and antiepileptics, which bind to the cavity of the internal entrance to the ion-conducting pore; (c) lipophilic voltage sensor trapping toxins, such as spider hanatoxin, which bind in the lipid membrane close to the extracellular end of S3; and, finally, (d) several newly discovered small-molecule compounds, such as the antiepileptic drug retigabine, which bind to the pore domain, thereby keeping the intracellular gate open. A central question is if PUFAs act on any of these four sites. Because PUFAs affect many voltage-gated ion channels with different primary structures (Boland and Drzewiecki, 2008), the PUFA action site is likely a common favorable lipophilic environment rather than a high-affinity lock-and-key site. Sites 3 and 4 above are both accessible via the lipid bilayer and are thus likely candidates.

Second, to better understand the interaction between the PUFA and the Kv channel, we also aimed to identify which step in the channel activation chain is affected by PUFA. A Kv channel is activated in several steps; that is, several molecular rearrangements precede channel opening (Zagotta et al., 1994; Schoppa and Sigworth, 1998; Keynes and Elinder, 1999; Börjesson and Elinder, 2008). In response to a positive voltage inside the cell, the four S4s first move independently of each other, from the intracellular side of the channel to the extracellular side. Subsequently, a final conformational change in S4 occurs, involving cooperativity between the VSDs, followed by opening of the ion-conducting pore. In theory, PUFAs could induce channel opening by affecting one or several of those activation steps.

We found that PUFA molecules affecting Kv channel voltage dependence act close to the lipid-facing outer halves of S3 and S4, representing a novel pharmacological site of action distinct from those reported previously for toxins (Swartz, 2007; Kopljar et al., 2009) and potential antiepileptics (Xiong et al., 2007; Blom et al., 2009; Lange et al., 2009). We also report that PUFAs act on the final voltage sensor transition and that the effect critically depends on specific amino acid residues at the outer end of S4, suggesting a channel specificity in the PUFA effect on ion channels. This offers the prospect of designing new channel-modifying compounds potentially useful in the treatment of epilepsy and heart arrhythmia, and may help design novel dietary regiments for alleviating these diseases.

MATERIALS AND METHODS

Molecular biology and channel expression

For the electrophysiological experiments, we expressed the Shaker H4 channel in *Xenopus laevis* oocytes. Residues 6–46 were deleted to remove fast inactivation (Hoshi et al., 1990). This channel is referred to as Shaker WT-IR throughout. The conducting ILT mutation (V369I/I372L/S376T) (Smith-Maxwell et al., 1998) and the nonconducting ILT mutation (referred to as ILT/W434F; C245V/V369I/I372L/S376T/C426A/W434F) were provided by E. Isacoff (University of California, Berkeley, Berkeley, CA). Frog surgery, oocyte handling, and cRNA injection (0.05–0.5 ng/oocyte for Shaker point mutants, 12.5 ng/oocyte for ILT mutant, and 33 ng/oocyte for ILT/W434F mutant) followed the procedures described previously (Börjesson et al., 2010). Animal experiments were approved by the local Animal Care and Use Committee

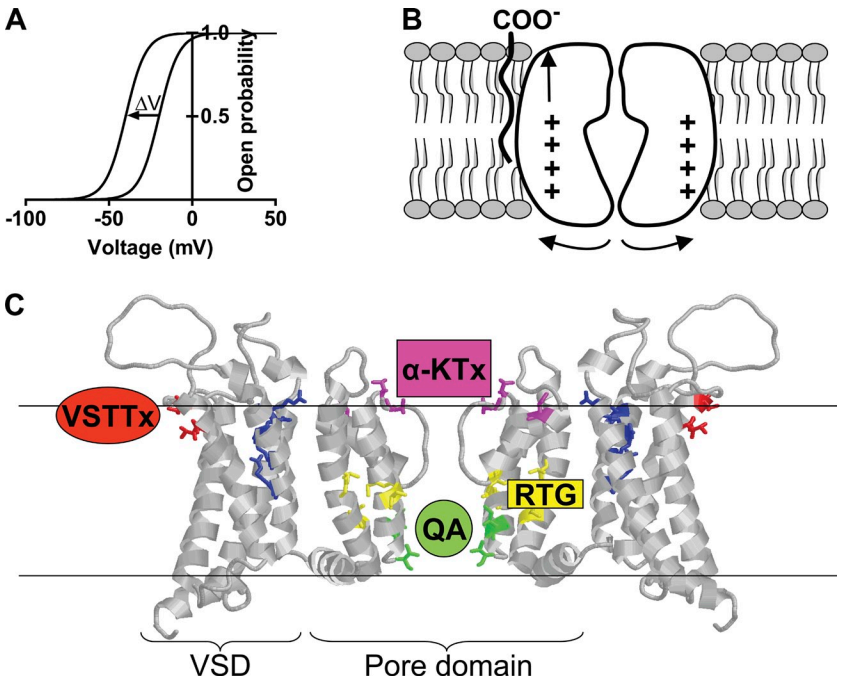

Figure 1. The lipoelectric mechanism and binding sites for other compounds. (A) Schematic illustration of the PUFA effect on the Shaker channel: negatively charged PUFAs shift the voltage dependence of a Kv channel in a negative direction along the voltage axis. (B) A PUFA binds with its hydrophobic acyl tail in the hydrophobic lipid bilayer or a hydrophobic pocket in the channel. From this position, the negatively charged carboxyl group of the PUFA electrostatically attracts the positively charged voltage sensor to open the intracellular gate of the ion channel. (C) Side view of the Kv1.2/2.1 chimera with Shaker side chains. Back and front domains are removed for clarity. Note that the VSDs and pore domains shown are from different subunits. Residues critical for quaternary ammonium compounds (Zhou et al., 2001) (I470 and V474 in green), pore-blocking toxins (MacKinnon et al., 1990) (D431, T449, and V451 in magenta), voltage sensor–trapping toxins (Swartz and MacKinnon, 1997) (L327, A328, and V331 in red), and retigabine (Lange et al., 2009) (I400, G406, V407, M440, and A464 in yellow) are shown as sticks. The gating charges R362, R365, R368, and R371 are marked as blue sticks. Residue numbering refers to Shaker.

at Linköping University. Cysteine point mutations were introduced using QuikChange Site-Directed Mutagenesis kit (Agilent Technologies) and verified by sequencing. cRNA for point mutants and ILT mutants was prepared using the mMessage mMachine T7 kit (Invitrogen).

Electrophysiological experiments

Ion and gating currents were measured 3–6 d after cRNA injection using the two-electrode voltage clamp technique (CA-1B amplifier; Dagan Corporation). Glass tips of borosilicate, filled with 3 M KCl, had a resistance of 0.5–2.0 MΩ. The holding voltage was −80 mV. Ion currents were measured at voltages between −80 and +60 mV (between +20 and +150 mV for the ILT mutant) in 5-mV increments. OFF gating currents of ILT/W434F were measured by first stepping to −120 mV (100 ms), then to prepulse voltages between −120 and +10 mV in 5-mV increments (100 ms), and finally to −100 mV (200 ms). All experiments were performed at room temperature (~20°C). The amplifier's leak and capacitive compensation were used, and the currents were low-passed filtered at 5 kHz. The control solution contained (in mM): 88 NaCl, 1 KCl, 15 HEPES, 0.4 $CaCl_2$, and 0.8 $MgCl_2$. pH was adjusted to 7.4, with NaOH yielding a final sodium concentration of ~100 mM. 4,7,10,13,16,19-all-cis-docosahexaenoic acid (DHA) was prepared, stored, and applied as described previously (Börjesson et al., 2008). DHA concentrations mentioned in this work are the effective concentrations, i.e., 70% of the nominal concentration (quantified in Börjesson et al., 2008).

Cysteine modification

A PUFA bound to the channel has an apparent pK_a value close to 7.4 (Börjesson et al., 2008). An alteration in the local pH close to the active PUFA alters the effect on the channel's voltage sensitivity by altering the proportion of deprotonated charged PUFA (Fig. 2 C; see also triple mutant in Börjesson et al., 2008). The local pH in turn depends on the fixed charges close to the PUFA. To alter the charge of the substituted cysteines, we used the cysteine-specific thiol reagents 2-aminoethyl methanethiosulfonate hydrochloride ($MTSEA^+$), [2-(trimethylammonium)ethyl] methanethiosulfonate bromide ($MTSET^+$), and sodium [2-sulfonatoethyl] methanethiosulfonate ($MTSES^-$; Toronto Research Chemicals). The MTS reagents were applied continuously to the bath solution using a gravity-driven perfusion system. The reagents were applied until full modification was achieved (typically 100 µM $MTSEA^+$, 100 µM $MTSET^+$, or 1 mM $MTSES^-$ for 200 s). The modification was assayed functionally in two-electrode voltage-clamped oocytes. The main substance used to introduce a positive charge at each mutated cysteine was $MTSEA^+$. The reason for using the smaller $MTSEA^+$ instead of the larger $MTSET^+$ is that we wanted a more defined charge localization and less steric effects than what is obtained from the larger reagents. $MTSEA^+$ can, in contrast to $MTSET^+$ and $MTSES^-$, pass the cell membrane (Holmgren et al., 1996) and was therefore first tested on Shaker WT-IR to identify possible interference from $MTSEA^+$ in the cytoplasm. 100 µM $MTSEA^+$ applied for >480 s had no effect on Shaker WT-IR (Table I). $MTSEA^+$ experiments were done at pH 7.4 because a higher pH would already from the beginning push the PUFAs toward a deprotonated state, and no further effect will be seen upon modification.

In addition to possible altered PUFA sensitivity upon $MTSEA^+$ modification, $MTSEA^+$ modification per se of a residue that is close to the voltage sensor can also induce electric and/or steric effects on channel activation. The electric and steric components for a charged MTS reagent can be derived by using differently charged MTS reagents (Broomand and Elinder, 2008). By also testing the effect of the negatively charged $MTSES^-$, the electric versus steric components can be quantified. The steric component is calculated as $\Delta V_{steric} = (\Delta V_{MTSES} + \Delta V_{MTSEA})/2$, and the electrostatic component is calculated as $\Delta V_{electric} = (\Delta V_{MTSEA} - \Delta V_{MTSES})/2$.

Analysis of data

The K conductance $G_K(V)$ was calculated as

$$G_K(V) = I_K / (V - V_{rev}), \quad (1)$$

where I_K is the steady-state current at the end of a 100-ms pulse, V is the absolute membrane voltage, and V_{rev} is the reversal potential for the K channel, set to −80 mV. The voltage dependence analysis and quantification of G-V shifts were done by measuring the shift at the 10% level as described previously (Börjesson et al., 2008, 2010) to avoid interference from endogenous currents and block by intracellular ions, as sometimes seen at the most positive voltages. For illustrative reasons, the figures presented here were generated by fitting a Boltzmann curve raised to the fourth power to the conductance data

$$G_K(V) = A(1 + \exp((V - V_{1/2})/s))^{-4}, \quad (2)$$

where A is the amplitude of the curve, and $V_{1/2}$ and s are the midpoint and the slope, respectively. s was constrained to a common value in each panel in the figures. After this fit, the data were normalized to $A = 1$. However, this procedure only marginally affected the amplitudes (<10%).

Q-V was analyzed by integrating the OFF gating current before and after DHA treatment. The gating charge was normalized and plotted against the prepulse voltage, and the control curve slid along the voltage axis until it overlapped the DHA curve.

Distance calculation

If a charge is located at the border between a low dielectric medium (the lipid membrane) and a high dielectric medium (water), the potential ψ(r) at the distance r from an elementary charge e_0 (e.g., the PUFA charge) can be calculated with a modified Coulomb's law (McLaughlin, 1989; Elinder and Århem, 2003),

$$\psi(r) = 2\, e_0 \exp(-\kappa\, r) / (4\, \pi\, \varepsilon_0\, \varepsilon_a\, r), \quad (3)$$

where ε_0 is the permittivity of free space (8.85×10^{-12} Fm^{-1}), ε_a is the relative dielectric constant of the aqueous phase (80), and κ is the inverse of the Debye length in the aqueous phase (9.8 Å in the 1-K solution; see e.g., Elinder et al., 2001b). Eq. 3 was used to get a rough estimate of the distance between the PUFA carboxyl charge and the gating charges in S4 based on DHA-induced Q-V and G-V shifts for the ILT mutant. The calculation is based on the assumptions that the surface of the channel is smooth, and that the top S4 charges pop up on the channel's surface one by one, leaving the interior of the channel unaffected with positive gating charges pairing with negative counter charges (see Fig. 6 A). This simple model has been evaluated previously (Elinder et al., 2001a) and proven surprisingly accurate (Elinder et al., 2001a; Broomand and Elinder, 2008).

Molecular K channel structure

The crystal structure of the Shaker channel is not determined. Therefore, we used the structure of the Kv1.2/2.1 chimera channel (Long et al., 2007) with Shaker side chains (provided by E. Lindahl, Royal Institute of Technology, Stockholm, Sweden) for the structural evaluations. The Kv1.2/2.1 chimera shares high sequence identity with the Shaker channel and has been shown previously to serve as an accurate Shaker model (Tao et al., 2010).

Kinetic modeling

For the computer simulations of K channel gating, we used a six-state model (Fig. 5 A). C_0 to C_4 indicate states of the channel with 0–4 activated voltage sensors (S4). The movements of the voltage sensors are independent of each other. From state C_4, the channel can open via a final cooperative step that involves all four subunits. The steady-state conditions are determined by α/β and by γ/δ, where

$$\alpha / \beta = \exp((V - V_{\alpha\beta})\, z_{\alpha\beta} F\, R^{-1}T^{-1}) \quad (4)$$

$$\gamma / \delta = \exp((V - V_{\gamma\delta})\, z_{\gamma\delta} F\, R^{-1}T^{-1}), \quad (5)$$

$V_{\alpha\beta}$ is the voltage where $\alpha = \beta$, $V_{\gamma\delta}$ is the voltage where $\gamma = \delta$, and $z_{\alpha\beta}$ and $z_{\gamma\delta}$ are the number of elementary charges moving through the membrane when the channel goes between two closed states or between C_4 and O, respectively. $V_{\alpha\beta}$ was set to −40 mV for WT-IR and −80 mV for ILT. $V_{\gamma\delta}$ was set to −40 mV for WT-IR and +100 mV for ILT. $z_{\alpha\beta}$ was set to 2 for both WT-IR and for ILT. $z_{\gamma\delta}$ was set to 1 for both WT-IR and for ILT. G-V and the gating charge versus voltage curve, Q-V, can easily be computed (see Fig. 5, F and G):

$$G(V) = \gamma / \delta / ((\alpha / \beta)^{-4} + 4(\alpha / \beta)^{-3} + 6(\alpha / \beta)^{-2} + 4(\alpha / \beta)^{-1} + 1 + \gamma / \delta) \quad (6)$$

$$Q(V) = 4z_{\alpha\beta}(\alpha / \beta)^{-3} + 12z_{\alpha\beta}(\alpha / \beta)^{-2} + 12z_{\alpha\beta}(\alpha / \beta)^{-1} + 4z_{\alpha\beta} + (4z_{\alpha\beta} + z_{\gamma\delta})\gamma / \delta) / ((\alpha / \beta)^{-4} + 4(\alpha / \beta)^{-3} + 6(\alpha / \beta)^{-2} + 4(\alpha / \beta)^{-1} + 1 + \gamma / \delta). \quad (7)$$

Statistical analysis

Average values are expressed as mean ± SEM. When comparing DHA-induced shifts of mutants with WT-IR, one-way ANOVA together with Dunnett's multiple comparison test was used. One-way ANOVA followed by Bonferroni's multiple comparison test was used to compare DHA sensitivity for each mutant before and after MTS modification. Mean values for MTS-induced shifts were analyzed using a two-tailed one sample t test, where mean values were compared with a hypothetical value of 0. $P < 0.05$ is considered as significant.

RESULTS

Cysteine mutations in the VSD but not in the pore domain affect the PUFA sensitivity

During previous investigations on the voltage-gated Shaker K channel, we found that some cysteine point mutations reduced the potency of the ω-3 PUFA DHA to affect the channel's voltage dependence compared with the Shaker WT-IR. Here, we have used DHA as the test substance but will refer to the effects as "PUFA effects" because we have found almost identical Shaker channel effects for six different investigated PUFAs, in sharp contrast to the lack of effects for monounsaturated, saturated, and methyl esters of fatty acids (Börjesson et al., 2008). In a previous investigation, we found that low concentrations such as 2 µM DHA had clear effects on the voltage dependence of the Shaker K channel (Börjesson et al., 2008), and that this small effect is expected to have substantial effects on excitability (X.P. Xu et al., 2008; Börjesson et al., 2010). In the present work, we aimed at detailing the interaction between DHA and the channel; therefore, much higher DHA concentrations (7–70 µM) were used.

We hypothesized that mutagenesis of residues close to the PUFA action site affects PUFA sensitivity more than distant residues do. Therefore, to localize this site, we

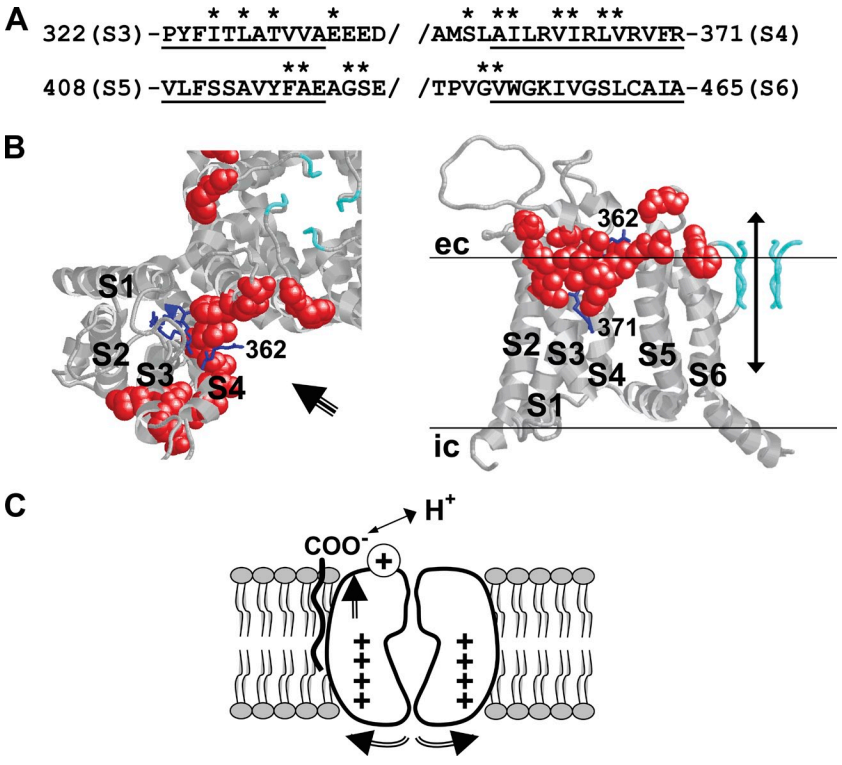

Figure 2. Strategy to determine the PUFA action site. (A) Sequence of segment S3–S6 for the Shaker K channel. //, the extracellular linkers are omitted; *, tested residues. Underlined residues mark helical transmembrane segments. (B) Structures of the Shaker K channel in an open state (based on the Kv1.2/2.1 chimera; Long et al., 2007). View from the extracellular side (left). Only one VSD and part of the pore domain are shown. View from the membrane side (right) as indicated by the arrow in the left panel. Only one VSD and the closest pore domain from another subunit are shown. Selectivity filter regions from all four subunits are displayed in cyan. The blue residues are the four most extracellular gating charges in S4 (R362, R365, R368, and R371). Red residues are explored in the present investigation. (C) Only the negatively charged form of the carboxyl group affects the voltage sensor. The effect is pH dependent. The introduction of a fixed positive charge close to the PUFA changes the local pH, deprotonates the carboxyl group, and potentiates the PUFA effect on the voltage sensor. The closer the charge is to the PUFA, the larger the potentiation is.

performed a systematic cysteine scan of a large surface of the channel based on the localization of the initial cysteine mutants. The point-mutated Shaker channels were then expressed in *Xenopus* oocytes and studied with two-electrode voltage clamp. 17 residues were selected for mutagenesis. The investigated residues are distributed over different segments of the channel (Fig. 2 A) and cover the lipophilic surfaces of the extracellular halves of S3, S4, S5, and S6 (Fig. 2 B, red residues). The reason for this selection is that PUFAs are lipophilic substances and thus prone to interact with residues facing a lipid environment, and they should be relatively close to the gating charges in the voltage sensor (Börjesson et al., 2008) (Fig. 2 B, blue sticks).

The ability of 70 µM DHA at pH 7.4 to shift the conductance versus voltage, G-V, curve along the voltage axis (as shown in Fig. 1 A) was tested for each cysteine mutant. Out of the 17 residues investigated, all but four mutants showed no alteration in DHA sensitivity (<1.6-mV deviation from the sensitivity of WT-IR; Table I). The four mutants with larger alterations in DHA sensitivity (>±2.8 mV) compared with WT-IR were I325C, T329C, I360C, and L366C. Residues I325C and T329C, located in the outer half of helix S3, had lost their sensitivity and were not significantly affected by DHA. I360C (located in S4) also showed reduced DHA sensitivity, but it was not statistically different from WT-IR in the one-way ANOVA analysis. L366C (in S4) displayed increased DHA sensitivity compared with WT-IR. The alterations in DHA sensitivity were not correlated with the minor alterations in the channels' voltage sensitivity caused by the mutation per se, denoted in Table I as the voltage for the 10% level of the G-V curve. These initial experiments suggested that residues in the VSD but not in the pore domain are important for PUFA acting on the channel's voltage dependence.

Positive charges close to the PUFA action site increase the PUFA potency

If the cysteine substitution of a residue induces only marginal changes in the side chain properties, the mutation will probably not alter the PUFA effect. Such cysteine mutants would thus incorrectly be interpreted as distant to the PUFA action site. Therefore, to further explore the critical area for PUFA action, we introduced a charge to each of the investigated residues. This charge can have three different effects on PUFA efficiency. (1) A positive charge close to the PUFA action site will increase the local pH and consequently deprotonate the PUFA molecule (Börjesson et al., 2008). This in turn will increase the PUFA effect on the channel's voltage dependence (Fig. 2 C). (2) A positive charge close to the PUFA action site will increase PUFA affinity and thereby increase PUFA effects at concentrations below saturating effects. (3) A positive charge located in the voltage sensor S4 moving toward the PUFA molecule promotes larger effects of the PUFA molecule on the voltage sensor movement. These three components can also work together, and we do not

TABLE I

Summary of cysteine point–mutated Shaker channels showing MTS-induced G-V shifts and DHA sensitivity before and after MTS modification

Channel	10% level	ΔV_{DHA}	p	ΔV_{MTSEA+}	p	ΔV_{DHA} (MTSEA$^+$)	$-\Delta\Delta V_{DHA}$	p	ΔV_{MTSES-}	p	ΔV_{DHA} (MTSES$^-$)	$-\Delta\Delta V_{DHA}$	p
	mV	*mV*		*mV*		*mV*	*mV*		*mV*		*mV*	*mV*	
WT-IR	−35.4 ± 0.7 (8)	−4.4 ± 0.9 (5)		−1.0 ± 1.0 (4)	0.4	−4.5 ± 0.6 (4)	−0.1	>0.05					
S3–S4													
I325C	−34.8 ± 1.3 (10)	−1.1 ± 1.4 (5)	<0.05	**+19.2 ± 1.1** (5)	<0.0001	−5.9 ± 0.5 (5)	**+4.8**	<0.001					
L327C	−31.4 ± 0.4 (6)	−4.3 ± 0.6 (3)	>0.05	**+7.0 ± 0.8** (3)	0.01	−5.1 ± 0.5 (3)	+0.8	>0.05					
T329C	−49.8 ± 0.6 (17)	−0.4 ± 0.6 (8)	<0.01	**+11.9 ± 0.4** (7)	<0.0001	−3.3 ± 0.3 (7)	**+2.8**	<0.05					
E333C	−40.0 ± 0.8 (16)	−2.9 ± 0.5 (6)	>0.05	+1.5 ± 0.8 (7)	0.1	−2.6 ± 0.5 (7)	−0.3	>0.05	**−4.0 ± 0.5** (3)	0.01	−4.3 ± 0.3 (3)	+1.4	>0.05
S357C	−30.0 ± 1.4 (12)	−5.3 ± 0.7 (4)	>0.05	**−21.7 ± 2.1** (4)	0.002	−3.3 ± 0.6 (4)	−2.0	>0.05					
A359C	−35.6 ± 0.6 (21)	−2.8 ± 0.5 (5)	>0.05	**+18.8 ± 2.0** (6)	0.0002	−7.3 ± 0.9 (6)	**+4.5**	<0.001					
I360C	−30.2 ± 1.3 (9)	−1.5 ± 0.4 (4)	>0.05	**+6.8 ± 0.9** (5)	0.002	−8.5 ± 1.5 (5)	**+7.0**	<0.001					
V363C	−38.8 ± 0.4 (8)	−3.4 ± 0.4 (4)	>0.05	**+1.8 ± 0.4** (4)	0.02	−3.1 ± 0.5 (4)	−0.3	>0.05					
I364C	−47.5 ± 0.6 (12)	−3.9 ± 0.5 (5)	>0.05	+0.6 ± 0.3 (5)	0.1	−3.5 ± 0.3 (5)	−0.4	>0.05	1.6 ± 1.1 (3)	0.3	−2.0 ± 0.8 (3)	−2.0	>0.05
L366C	−50.0 ± 1.0 (19)	−7.7 ± 1.7 (7)	<0.05	−2.0 ± 1.4 (5)	0.2	−4.5 ± 0.3 (5)	**−3.2**	<0.05	−0.4 ± 0.5 (6)	0.5	−4.1 ± 0.8 (6)	**−3.5**	<0.01
V367C	−53.5 ±0.8 (18)	−3.1 ± 0.2 (5)	>0.05	−3.9 ± 2.5 (9)	0.2	−3.9 ± 0.5 (9)	+0.8	>0.05	**+0.4 ± 0.1** (4)	0.04	−4.0 ± 0.5 (4)	+0.9	>0.05
S5–S6													
F416C	−39.4 ± 0.7 (19)	−3.5 ± 0.7 (7)	>0.05	**+26.9 ± 0.6** (8)	<0.0001	−4.4 ± 0.9 (5)	+0.9	>0.05	**+3.7 ± 0.3 (4)**	0.002			
A417C	−34.7 ± 0.8 (10)	−4.3 ± 0.4 (5)	>0.05	**−1.4 ± 0.5** (5)	0.04	−4.2 ± 0.1 (5)	−0.1	>0.05					
G420C	−32.1 ± 0.9 (16)	−3.2 ± 0.4 (5)	>0.05	+1.5 ± 1.3 (7)	0.3	−4.8 ± 0.9 (7)	+1.6	>0.05	−0.7 ± 0.4 (5)	0.2	−4.8 ± 0.2 (5)	+1.5	>0.05
S421C	−34.7 ± 0.5 (23)	−4.2 ± 0.2 (6)	>0.05	**+2.9 ± 0.6** (8)	0.001	−6.2 ± 0.6 (8)	+2.1	>0.05					
G452C	−39.0 ± 1.2 (11)	−3.9 ± 0.3 (5)	>0.05	**+5.4 ± 0.8** (6)	0.0008	−6.0 ± 0.6 (6)	+2.1	>0.05					
V453C	−38.8 ± 1.4 (12)	−4.4 ± 0.5 (6)	>0.05	**+5.2 ± 0.8** (6)	0.002	−5.4 ± 0.3 (5)	+1.0	>0.05					

70 µM DHA, 100 µM MTSEA$^+$, and 1 M MTSES$^-$ were used. Data are expressed as mean ± SEM, with *n* denoted in parenthesis. Underlined data mark mutants with altered DHA sensitivity compared to WT-IR. Statistically significant MTS-induced ΔV or $\Delta\Delta V_{DHA}$ are in bold.

aim at quantifying the impact of each component. What is important is that in all three cases, high-impact residues should be close to the PUFA action site. A change in PUFA potency, independent of the underlying mechanism, is therefore our readout to indentify high-impact residues. To experimentally change the charge of each mutated cysteine, we modified the cysteine with the positively charged cysteine-specific reagent $MTSEA^+$. This modification of a residue that is close to the voltage sensor will electrostatically shift the G-V curve in a positive direction along the voltage axis, in addition to any steric effect on channel activation. The closer to the voltage sensor, the larger the expected electrostatic effect is (Elinder et al., 2001a; Broomand and Elinder, 2008). For these experiments, we used pH 7.4 because the charge-induced effects are expected to be larger close to the

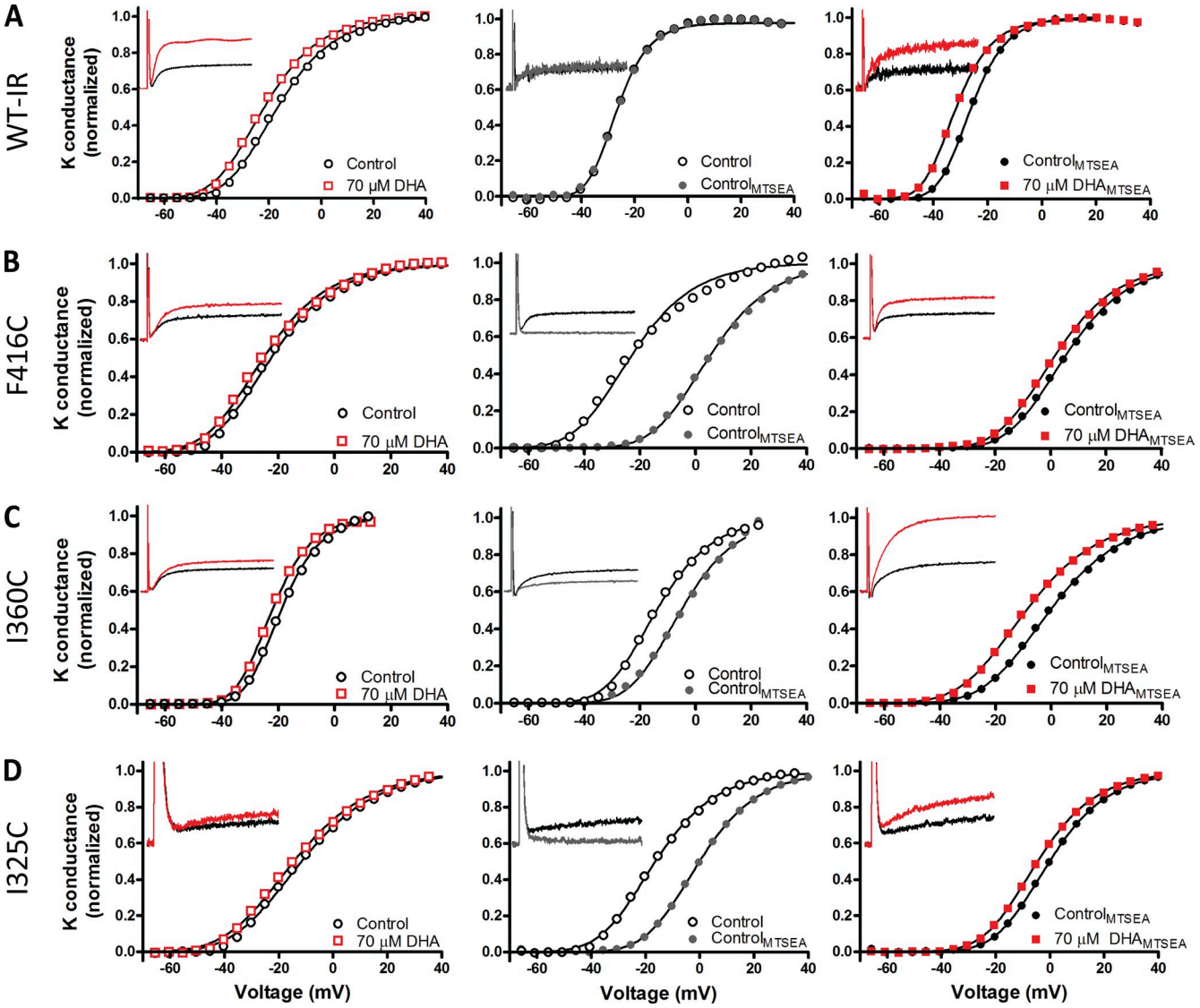

Figure 3. Effects of DHA and $MTSEA^+$ at pH 7.4 on WT-IR and three mutations. Graphs display representative G-V curves with current traces as insets for voltages corresponding to 10% of G_{max} in control solution. Eq. 2 is used for the fit. (A) Data for WT-IR. 70 μM DHA shifts the control curve for WT-IR with −4.7 mV (left). $V_{1/2}$ = −42.8 and −47.5 mV, and s = 16.1 mV. $MTSEA^+$ modification does not shift the control curve (middle). $V_{1/2}$ = −38.9 and −38.9 mV, and s = 7.4 mV. The DHA-induced shift is not affected by $MTSEA^+$ modification (right). $V_{1/2}$ = −39.7 and −45.4 mV, and s = 8.2 mV. (B) Data for F416C. 70 μM DHA shifts the control curve for F416C with −2.8 mV (left). $V_{1/2}$ = −45.7 and −48.5 mV, and s = 14.0 mV. $MTSEA^+$ modification shifts the control curve with +28.2 mV (middle). $V_{1/2}$ = −46.2 and −18.0 mV, and s = 14.0 mV. The DHA-induced shift is not affected by $MTSEA^+$ modification (right). $V_{1/2}$ = −18.0 and −21.8 mV, and s = 14.0 mV. (C) Data for I360C. 70 μM DHA shifts the control curve for I360C with −3.1 mV (left). $V_{1/2}$ = −33.5 and −36.6 mV, and s = 8.7 mV. $MTSEA^+$ modification shifts the control curve with +8.8 mV (middle). $V_{1/2}$ = −34.7 and −25.9 mV, and s = 12.4 mV. The DHA-induced shift is increased to −8.5 mV after modification (right). $V_{1/2}$ = −27.3 and −35.8 mV, and s = 16.1 mV. (D) Data for I325C. 70 μM DHA shifts the control curve for I325C with −2.9 mV (left). $V_{1/2}$ = −40.1 and −43.0 mV, and s = 17.2 mV. $MTSEA^+$ modification shifts the control curve with +16.9 (middle). $V_{1/2}$ = −39.4 and −22.5 mV, and s = 13.7 mV. The DHA-induced shift is increased to −4.4 after modification (right). $V_{1/2}$ = −22.6 and −27.0 mV, and s = 13.5 mV.

apparent pK_a value. Control experiments showed that WT-IR was not affected by $MTSEA^+$ (Fig. 3 A).

Residues in the pore domain are close to the voltage sensor but distant from the PUFA action site

Residue 416 is located at the extracellular end of S5 at atomic distance to the top charge of S4 (residue R362) in the open state (Broomand et al., 2003; Lainé et al., 2003). 70 µM DHA at pH 7.4 shifts the G-V curve for F416C with −3.5 mV (Fig. 3 B, left, and Table I), which is close to what has been found for WT-IR (Fig. 3 A, left, and Table I). When modifying F416C with $MTSEA^+$, the G-V curve was shifted +27 mV (Fig. 3 B, middle, and Table I), suggesting that F416 is very close to the voltage sensor if the induced shift is of electrostatic origin. To estimate the electrostatic component of this shift, we also modified F416C with the negatively charged $MTSES^-$ (Elinder et al., 2001a). The electrostatic component was 11.6 mV (see Materials and methods for calculations), which means that a charge at position 416 electrostatically affects the voltage sensitivity with 11.6 mV, suggesting that residue 416 is located a short distance (∼10 Å; Eq. 3) from the voltage sensor, as shown previously (Broomand et al., 2003; Lainé et al., 2003). To find out if 416 is also close to the PUFA action site, we tested if the PUFA-induced shift was enhanced by the $MTSEA^+$ modification. The PUFA-induced shift was not significantly different from the unmodified channel or the WT-IR channel (Fig. 3 B, right, and Table I). Three similar examples are S421C, G452C, and V453C, all located in the pore domain at the top of S5 and S6, respectively (Table I). This is consistent with the top of S5 and S6 being close to the voltage sensor S4, but it also suggests that the pore domain is distant from the PUFA action site. One of the residues we investigated in the pore domain, G420C did not show any alterations ($MTSEA^+$, $MTSES^-$, or changes in DHA response). Either it is buried from the extracellular solution and thus not modified, or it is pointing away from both the voltage sensor and the PUFA action site.

Residues in S3 and S4 are both close to the voltage sensor and to the PUFA action site

Of 11 investigated residues in S3–S4, 10 were modified by either $MTSEA^+$ or $MTSES^-$ as judged either directly by a change in the channel's voltage sensitivity or indirectly by a change in the channel's DHA sensitivity (Table I). Only residue I364C was not affected by the MTS reagents, suggesting a buried position not exposed to the extracellular solution. 4 of the 10 modified residues (I325C, T329C, A359C, and I360C) increased their sensitivity to DHA when the residues were made positively charged by $MTSEA^+$.

For I360C, located two residues outside the first gating charge in S4, and for I325C, in S3, 70 µM DHA at pH 7.4 shifts the G-V with −1.5 and −1.1 mV, respectively (Fig. 3, C and D, left, and Table I). For both mutations, modification with $MTSEA^+$ clearly shifts the G-V with +7 and +19 mV, respectively (Fig. 3, C and D, middle, and Table I). The $MTSEA^+$ modification significantly increased the DHA-induced shift to −8.5 and −5.9 mV, respectively (Fig. 3, C and D, right, and Table I), clearly more than for WT-IR. Therefore, both residues 325 and 360 are suggested to be located in or close to the voltage sensor (as also found in the structure) and to the PUFA action site. $MTSEA^+$ modification of T329C in S3 and A359C in S4 also significantly affected the voltage sensitivity of the channel and the PUFA-induced shift (Table I). This is consistent with the cysteine mutagenesis data (see above); the three cysteine mutations that significantly altered the DHA sensitivity (325C, 329C, and 366C) are geographically close to or overlap with the residues that increase their DHA sensitivity when charge modified (325C, 329C, 359C, and 360C). Examination of the molecular structure showed that high-impact residues are clustered in a small region of the lipid-facing S3–S4 corner of the VSD (Fig. 4 A). An estimation of the PUFA action site locates the PUFA carboxyl charge in the lipid bilayer adjacent to S3 and S4 (Fig. 4, A and B). Intriguingly, this is the same motif on the channel as membrane phospholipids are suggested to interact with to alter channel gating (Milescu et al., 2009).

Strategy to analyze which step in the activation chain is affected by PUFA

So far, we have localized the PUFA action site to the periphery of the Shaker K channel close to S3 and S4, distant from the pore region. This also suggests that PUFA affects the movement of S4, rather than movements in the pore domain associated with the channel opening. However, it is not clear which steps in the activation chain are affected. A simple five-step model can be used in the analysis of the channel opening (Fig. 5 A). It is generally agreed that the activation can be divided into two main components. (1) The first component is independent outward movements of the four S4 helices (corresponding to the four steps from C_0 to C_4). In reality, each S4 moves in several steps (Zagotta et al., 1994; Keynes and Elinder, 1998b; Schoppa and Sigworth, 1998; DeCaen et al., 2009), but for simplicity, we fuse these early transitions to a single step in each subunit. (2) When all S4s are in an activated position (Fig. 5 A, C_4), the channel can open via a final voltage-dependent step in which all S4s move together (Sigg et al., 1994; Zagotta et al., 1994; Keynes and Elinder, 1998a; Schoppa and Sigworth, 1998; Ledwell and Aldrich, 1999; Pathak et al., 2005). The final S4 movement affects the pore domain to open the channel (Pathak et al., 2005). All steps in the model are voltage dependent, but most of the voltage dependence comes from the early steps (representing 80–85% of the gating charges compared with only 15–20% in the final step; Schoppa et al., 1992). The PUFAs could affect the voltage dependence of the opening either by

affecting only the early steps, only the final step, or both types of steps.

In a previous investigation (Börjesson et al., 2008), we found larger PUFA effects on the ion currents than on the gating currents (mainly generated by the C_0–C_4 steps), suggesting that the opening step is more affected than the early transitions. However, the exact relation was difficult to resolve because it depends on the type of model used for Kv channel gating. To better quantify the PUFA effect on the different activation steps, we used the ILT mutant Shaker channel where three hydrophobic residues in S4 are substituted for three other hydrophobic residues (V369I, I372L, and S376T). The ILT mutation separates the early steps from the final step, which are then possible to study in isolation (Smith-Maxwell et al., 1998). The early transitions occur at voltages around −80 mV, whereas the opening occurs around +50 mV (see Fig. 5 B). Thus, the G-V in the ILT mutant only reports on the opening step, with no involvement of the early transitions. If the W434F pore mutation is introduced, occluding the pore with no effects on the voltage sensor movement (Perozo et al., 1993), we instead get information of the early steps in isolation. The ILT experiments were performed at pH 9.0 to make sure that the fatty acid is fully charged and to induce as large PUFA effects as possible for robust quantification; the pK_a value for a fatty acid incorporated in the membrane is ∼7.4 (Rooney et al., 1983; Börjesson et al., 2008).

PUFA mainly affects the final opening step, with minor effects on the early transitions

First, we investigated the ion-conducting ILT mutant, which directly reports on the opening of the channel. DHA had a large effect on this K current (Fig. 5 C). 70 µM DHA at pH 9.0 increased the current at +60 mV by a factor of ∼10. DHA clearly shifted the G-V curve in the negative direction along the voltage axis (Fig. 5 D), qualitatively similar as the DHA-induced G-V shift for WT-IR. However, the shift was larger for ILT than for WT-IR. At pH 9.0, 70 µM DHA shifted G-V for ILT with −30 ± 2.5 mV (n = 5), whereas G-V for WT-IR was shifted −18 ± 1.4 mV (wild-type data from Börjesson et al., 2008). The larger effect on the G-V for the ILT mutant than for the WT-IR channel suggests that the opening step is more affected than the early steps. In the WT-IR channel, a large effect on the opening step is probably masked by much smaller effects on the early steps, which kinetically interfere with the opening step.

Second, to quantify the effects on the early steps, we also studied gating currents in the ILT/W434F mutant. DHA had a much smaller effect on the gating currents, Q-V, than on the conductance (Fig. 5, E and H). At pH 9.0, 70 µM DHA shifted Q-V for ILT/W434F with −5.0 ± 0.8 mV (n = 3; Fig. 5 E). Even though this effect on the gating currents is much smaller than that for the opening step, it suggests that the early transitions are also affected in the Shaker K channel. Fig. 5 H summarizes shift data for G-V and Q-V for both WT-IR and ILT (open bars). The smaller effect on G-V and the larger effect on Q-V for the WT-IR channel compared with ILT suggest that, under the assumption that the ILT mutation does not alter the relation of the DHA effects on the early and the late steps, the opening step and the major gating charge steps kinetically affect each other in WT-IR.

A simple gating model is quantitatively consistent with the experimental data

To quantitatively evaluate the experimental DHA data for the two activation steps, we used a simple gating model (Fig. 5 A and Eqs. 4–7). To mimic the effects of 70 µM DHA at pH 9.0, we shifted the voltage dependence of the first transitions ($V_{\alpha\beta}$ for C_0–C_4) with −5 mV, as experimentally found for Q-V for ILT/W434F, and the voltage

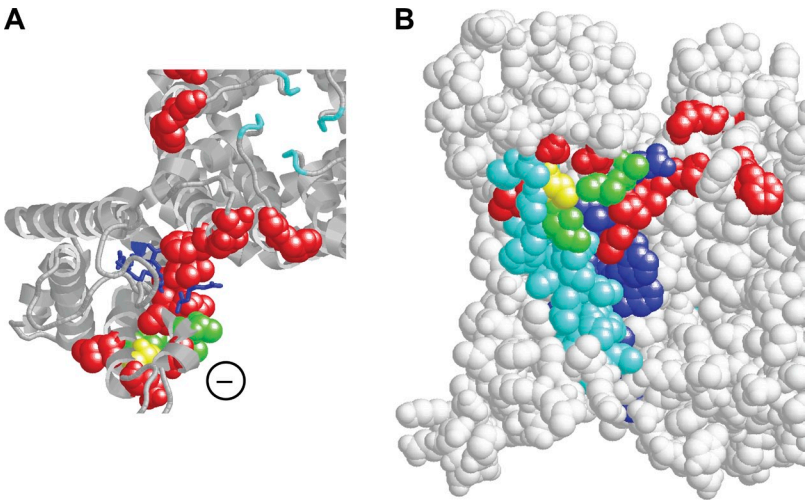

Figure 4. Localization the PUFA action site. (A) Extracellular view of the Shaker K channel in an open state (based on the Kv1.2/2.1 chimera; Long et al., 2007). Only one VSD and part of the pore domain are shown. The blue residues are the four most extracellular gating charges (R362, R365, R368, and R371). The selectivity filter is shown in cyan. Green residues (I325, A359, and I360) have the largest impact on the PUFA-induced shift of the G-V curve, the yellow residue (T329) has a smaller but significant effect on the PUFA-induced shift, and red residues have no significant effects on the PUFA-induced shifts. The negative charge denotes an approximate position of the PUFA carboxyl charge affecting the voltage sensitivity of the Shaker K channel. (B) Side view of the channel with I325, A359, and I360 in green, T329 in yellow, and residues with no significant effects on the PUFA-induced shifts in red. Not investigated residues in S3 are shown in cyan, and those in S4 are shown in blue. All residues in space fill.

dependence for the opening step ($V_{\gamma\delta}$) with −30 mV, as experimentally found for the G-V shift for the ILT mutant (Fig. 5, F and G, for computations). The effect on the voltage dependence of the computed Q-V and G-V curves for wild-type and the ILT mutant induced by these shifts was subsequently measured. A summary of all experimental and computational shifts is shown in Fig. 5 H. The concordance between experimental and computational data is striking, suggesting that DHA affects the first activation steps with −5 mV and the final opening step with −30 mV.

Horizontal charge movement of R1 explains the differential effects on the early and the final transitions

A helical-screw motion of S4 (Catterall, 1986; Guy and Seetharamulu, 1986; Broomand and Elinder, 2008) suggests that the positive gating charges emerge one by one on the channel's surface during activation (Keynes and Elinder, 1999; Elinder et al., 2001a). In the closed state C_0, none of the gating charges in S4 are exposed on the surface, whereas in the open state O, the three outermost arginines, R1–R3, are exposed to the extracellular solution (Fig. 6 A) (Baker et al., 1998; Keynes and Elinder, 1999; Long et al., 2007; Börjesson and Elinder, 2008). In the last closed state C_4, with all S4s in an activated but nonconducting position, we suggest that R1 and R2 are exposed to the extracellular solution with its charges at a distance of 16 Å away from the approximate PUFA position in the lipid bilayer adjacent to S3 and S4 (Fig. 6 B, green and orange residues; note that the color coding in Fig. 6 A corresponds to the color coding for the suggested position of R1 in Fig. 6 B). It has been suggested

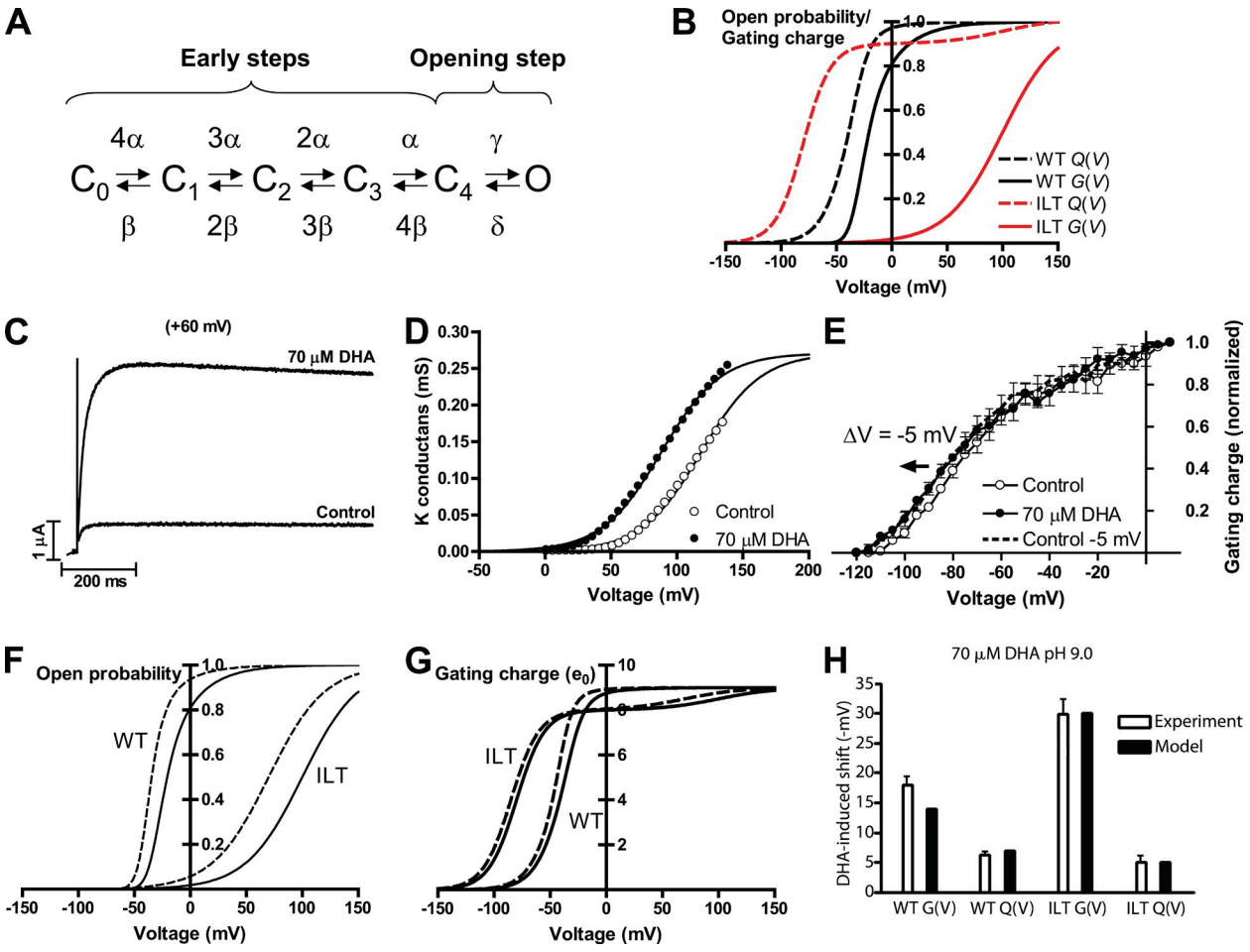

Figure 5. Effect of DHA on the early activation steps versus the opening step. (A) A simple scheme for the ion channel kinetics. C_0 to C_4 denote closed states with 0–4 activated voltage sensors where the voltage sensors move independently of each other. O is the open state. (B) Theoretical G-V curves and Q-V curves for WT-IR and the ILT channel generated from the model in A. For calculations, see Eqs. 4–7 in Materials and methods. (C) 70 µM DHA at pH 9.0 increases the ion current at +60 mV in the ILT channel. Holding voltage is −80 mV. (D) The G-V curve is shifted −30 mV for the ILT channel. Eq. 2 is fitted to the experimental data as explained in Materials and methods. $V_{1/2}$ = 118 mV for control and 88 mV for DHA. s = 22.6 mV and A = 0.271 mS in both curves. (E) Integrated OFF gating currents from the ILT/W434F mutation (n = 3). 70 µM DHA at pH 9.0 shifts the control curve −5 mV. (F and G) Calculated effects of DHA on open probability (F; G-V) and gating charge movement (G; Q-V) using Eqs. 4–7. Continuous lines are control curves. Dashed curves are DHA-affected curves. DHA was set to shift $V_{\alpha\beta}$ with −5 mV and $V_{\gamma\delta}$ with −30 mV for both channels. (H) Summary of DHA-induced shifts from both experiments and models. Data are expressed as mean ± SEM (n = 3–9).

that S4's final transition opens the channel (Keynes and Elinder, 1998a; Pathak et al., 2005; Phillips and Swartz, 2010). Assuming that the final position of S4 is according to the Kv1.2/2.1 chimera crystal structure, the charge of R1 moves to a position only 6 Å away from the PUFA when the channel is open (Fig. 6 B, red residue).

Can this structural hypothesis quantitatively explain our data? In previous work, we have successfully and with high accuracy used electrostatic equations (Eq. 3 in the present work) to determine distances at the surface of the Shaker K channel (Elinder et al., 2001a; Broomand and Elinder, 2008). Eq. 3 gives the change in surface potential as a function of distance from a charge, and it was used here to estimate the distance between the PUFA carboxyl charge and S4. Of course, the PUFA carboxyl charge will electrostatically interact with all charges in the channel. However, in a helical screw–like model, each step in the activation pathway is equivalent to removing the bottom charge of S4 and adding an S4 charge at the extracellular surface (Fig. 6 A, dashed arrows). Assuming a helical-screw motion of S4, the only electrostatic effect of PUFA on the channel, for each step in the activation pathway, is the interaction of PUFA with the added S4 charge on the extracellular surface (under the assumption that the interaction with the removed bottom S4 charge is negligible). All other PUFA–channel electrostatic interactions cancel each other because each S4 charge is replaced by the next S4 charge in a helical-screw model, and conserved negative counter ions always pair up with the gating charges within the electric field. Based on these assumptions, the 5-mV effect on the first S4 steps suggests that the PUFA charge is located 15.2 Å away from the position where the positive charges emerge on the channel protein's surface. This is very close to the structural prediction of 16 Å. The 30-mV effect on the opening step suggests that the PUFA charge is located 6.3 Å away from R1 in the open state, which again is almost identical to our prediction from the structural model. Collectively, our experimental data combined with the presented calculations suggest that R1 and R2 are exposed to the extracellular solution at a distance of ∼16 Å from the PUFA action site in the final closed state, C_4. In the opening step (from C_4 to O), R1 translates along the longitudinal axis of S4 and swings around the S4 helix toward the head groups of the lipid bilayer, close to the location of the charge of the bound PUFA (∼6 Å).

Charge mutations in S4 suggest channel-specific effects of PUFA on channel gating

The above mentioned structural model, where R1 moves from a position ∼16 Å away from the PUFA charge to a position only ∼6 Å away during the opening step, implies that the positive charge at R1 is critical for the

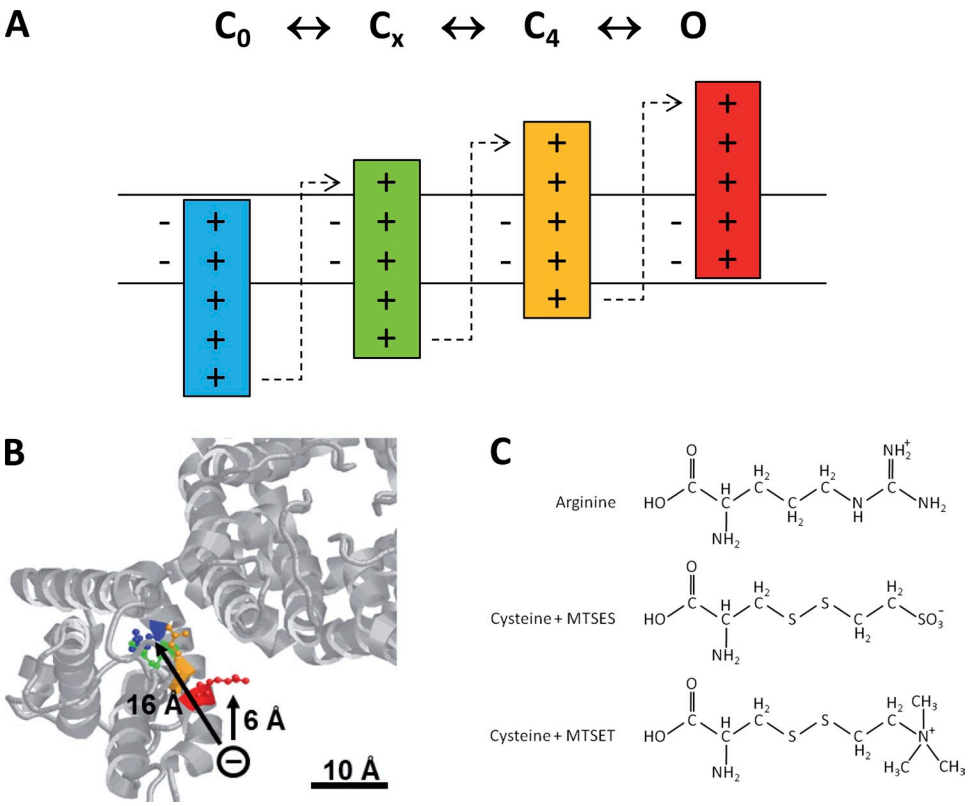

Figure 6. Strategy to test if PUFA facilitates horizontal S4 movement. (A) Schematic illustration of the assumed charge-transfer motion used for distance calculations (Eq. 3). The only change in electric charges between each gating state is that one gating charge is moved from the intracellular side to the extracellular side. Gating charges within the membrane electric field pair up with conserved negative charges. (B) Structure of the Shaker K channel in the open state (based on the Kv1.2/2.1 chimera). One VSD and part of the pore domain are shown. The four most extracellular-positive charges in S4 are colored: red, R362; orange, R365; green, R368; blue, R371. The negative charge denotes the position for the effective PUFA molecule. Arrows denote the distances from the effective PUFA site to the charge of R362 and to the site where the positive charges of R365 and R368 emerge on the surface, respectively. (C) Structural comparison of an arginine, a $MTSES^-$-modified cysteine, and a $MTSET^+$-modified cysteine.

effect of PUFAs. If the PUFAs interact electrostatically with R1 to promote opening, a negative charge at R1 would instead be expected to reduce or even reverse the PUFA effect. To alter the charge of R1 without altering the size of the side chain, we changed the arginine to a cysteine and modified with differently charged MTS reagents (Fig. 6 C): negatively charged $MTSES^-$ (mutant called $R362^-$; Fig. 7 B) and positively charged $MTSET^+$ (mutant called $R362^+$; Fig. 7 C). These experiments were performed at pH 9.0 to promote a negative charge of the carboxyl group of DHA, avoiding changes in the charge of the DHA (pK_a = 7.4; Börjesson et al., 2008) as a result of possible changes in local pH caused by the differently charged MTS reagents. In the same investigation, we showed that introducing three positive charges close to the voltage sensor only affected the local pH with 0.3 pH units.

7 µM DHA at pH 9.0 reduced, rather than increased, the current at −35 mV for $R362^-$ and induced a small but significant G-V shift in depolarizing direction (+2.3 ± 0.6 mV; n = 5; Fig. 7 B). This experiment suggests that DHA, despite the electrostatic repulsion from the

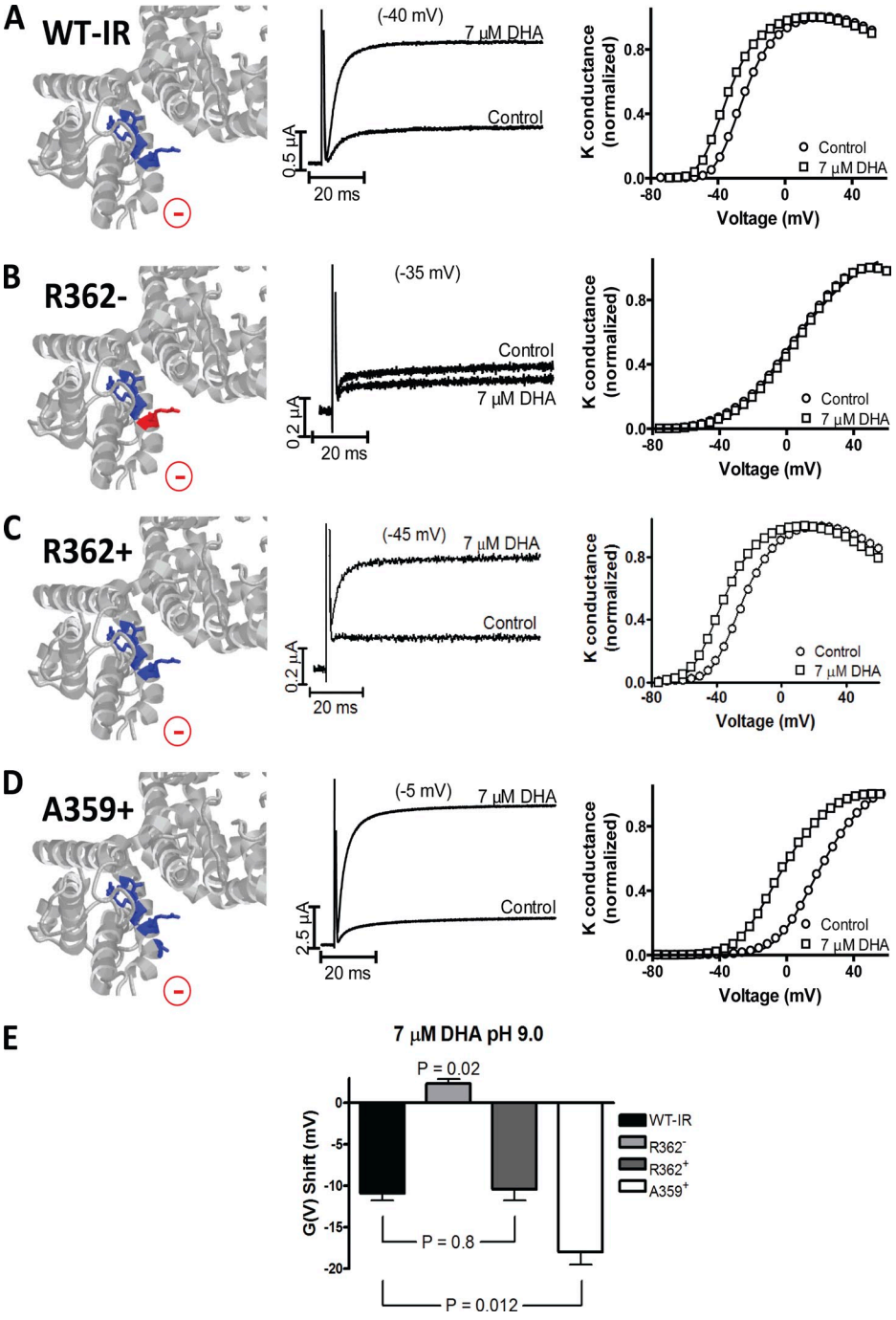

Figure 7. Effect of gating charge mutations on DHA sensitivity. (A) Data for WT-IR. Structure of the Shaker K channel in the open state (based on the Kv1.2/2.1 chimera), with residues R362, R365, R368, and R371 in blue (left). One VSD and part of the pore domain are shown. Current traces at −40 mV (middle) and G-V curve fitted to Eq. 2 (right). $V_{1/2}$ = −43.5 and −53.2 mV, and s = 11.3 mV. (B) Data for $R362^-$. Residue R362 are shown in red, and residues R365, R368, and R371 are shown in blue (left). Current traces at −35 mV (middle) and G-V curve fitted to Eq. 2 (right). $V_{1/2}$ = −36.8 and −34.9 mV, and s = 25.9 mV. (C) Data for $R362^+$. Residues R362, R365, R368, and R371 are shown in blue (left). Current traces at −45 mV (middle) and G-V curve fitted to Eq. 2 (right). $V_{1/2}$ = −45.9 and −58.3 mV, and s = 13.1 mV. (D) Data for $A359^+$. Residues A359, R362, R365, R368, and R371 are shown in blue (left). Current traces at −5 mV (middle) and G-V curve fitted to Eq. 2 (right). $V_{1/2}$ = −9.5 and −33.0 mV, and s = 18.1 mV. (E) Summary of experimental data for gating charge mutants. Data are expressed as mean ± SEM (n = 4–9).

negatively charged 362 residue, finds it attractive to bind to a site close to S3/S4. In contrast, $R362^+$ restored the PUFA sensitivity (Fig. 7 C), giving similar G-V shifts as for WT-IR (Fig. 7 A). The structural model also suggests that an additional gating charge at position 359 (one turn above R1, also called R0) could further potentiate the PUFA effect by providing an extra charge for the PUFA to interact with. Indeed, when attaching $MTSET^+$ to A359C ($A359^+$) at pH 9.0, the DHA-induced G-V shift was increased from −11 to −18 mV (Fig. 7 D). For this channel, 2.1 µM DHA in its deprotonated form shifted the G-V with as much as −6.4 ± 0.4 mV (n = 3), reinforcing the idea that a channel with a positive charge at R0 can be very much affected by physiological concentrations of DHA. Fig. 7 E summarizes the charge-modifying data for R1 and R0, suggesting that PUFAs influence the voltage dependence of the opening step mainly by interacting electrostatically with the outer end of S4. The experiments changing the charge of R0 and R1 (a) support the proposed localization of the PUFA action site, (b) suggest that it is a final S4 transition moving the outermost gating charge toward the lipid bilayer that underlies the actual opening step, and (c) suggest that PUFAs should have very different effects on different ion channels depending on the presence of a charge at positions R0 and/or R1. This last insight highlights the selective effects on different ion channels and opens up the development of future medical drugs selectively affecting neuronal and cardiac excitability.

DISCUSSION

In this study, we have localized the site of action for PUFAs affecting the voltage dependence of the Shaker K channel to a position in the lipid bilayer close to the extracellular halves of S3 and S4 in the VSD. We have also found that DHA mainly affects the final S4 transition, which is closely linked to the channel opening.

Several models for S4 motion are consistent with the PUFA data

A tilted helical-screw motion in three steps (Keynes and Elinder, 1999; Tiwari-Woodruff et al., 2000; Lecar et al., 2003) is consistent with all of our experimental data (Fig. 8 A, top), but variations on the same theme could also explain the data: a helical-screw motion followed by a tilt of S4 in the final step (Pathak et al., 2005) (Fig. 8 A, middle), and a translational motion of a 3_{10} helix followed by a 3_{10}-to-α-helix conversion in the final step (Shafrir et al., 2008; Bjelkmar et al., 2009; Schow et al., 2010) (Fig. 8 A, bottom). A small electrostatic PUFA effect on the early S4 movements (C_0 to C_4) can easily be understood from a simple surface charge theory, in which the PUFA carboxyl group provides additional fixed negative charges on the extracellular surface. If the charge is located close to the VSD, the modified transmembrane field will be sensed by the voltage sensor, and a smaller depolarizing step is needed to open the channel (Elinder and Århem, 2003). The mechanism is the same for all models. The larger PUFA effect on the opening step can be explained in a similar way if voltage sensor charges are moving closer to the PUFA action site during the opening step ($C_4 \rightarrow O$). This occurs in all described models (Fig. 8 A). A gating charge movement in the plane of the membrane is also supported by the finding that a charge at R1 and R0 has profound effects on the PUFA potency. Such a model also implies the possibility that the PUFA affinity might be state dependent: a higher affinity in the open state than in a closed state. However, this has not been tested in the present investigation. These data are in concordance with fluorescence measurements suggesting that S4 moves laterally, with only a smaller transmembrane component, during the opening step (Pathak et al., 2005). The exact VSD rearrangement underlying the opening step is not known; therefore, it is difficult to differentiate between the models in Fig. 8 A. However, a recent investigation shows that the top charge of S4, R1, moves in an outward direction from the membrane during the final transition (Phillips and Swartz, 2010), thus supporting the helical-screw model in the top panel of Fig. 8 A.

A new site and a new mechanism

Does the PUFA action site reported in this investigation overlap with the site for other compounds (Fig. 1 C), and is the mechanism similar? We conclude that the PUFA action site (Fig. 8 B, orange) does not overlap with binding sites for other compounds. We also conclude that the mechanism of action for the PUFAs is unique. Kv channel openers are rare, but shifts in the voltage dependence similar to those induced by PUFAs are seen for a few synthetic compounds (for example, retigabine, ZnPy, and acrylamide on the Kv7.2/3 channel). However, these substances stabilize the open-channel conformation through interactions with distinct sites in the pore domain (Fig. 8 B, yellow residues) (Xiong et al., 2007; Blom et al., 2009; Lange et al., 2009) and not through interactions with the VSD. Also, the ciguatera toxin gambierol interferes with Kv channel gating (Kopljar et al., 2009) by binding to the lipid-exposed surface of the pore domain and stabilizing the closed channel.

Other compounds bind to the VSD to trap the channel in a certain conformation. Voltage sensor–trapping toxins bind to the outer part of S3 and the S3–S4 linker (Fig. 8 B, red residues) and trap the channel in an open or closed conformation depending on which conformation provides the highest toxin affinity (Swartz, 2007; Börjesson and Elinder, 2008). Lipophilic toxins and PUFAs demonstrate the diversity of molecules that can access the channel via the surrounding membrane. NH29 binds in a water-exposed crevice in the VSD and stabilizes the open channel through interactions with S2 and

S4 (Peretz et al., 2010). The voltage sensor–trapping toxin site is close to the PUFA action site (the NH29 site is slightly more distant), but the mechanism for trapping is suggested to be of steric origin and thus different from the electrostatic PUFA mechanism. To our knowledge, this is the first report of a gating-modulating drug that electrostatically affects the voltage sensor to promote the final opening step. The beauty of the mechanism is that both reduced and increased excitability can be reached depending on the charge of the substance (Börjesson et al., 2008, 2010).

We would like to stress that the PUFA action site reported in this work was identified by studying the ability of PUFAs to change Shaker channel voltage dependence and is therefore the site of action for PUFAs acting by the lipoelectric mechanism. This does not exclude the presence of other PUFA–channel interfaces affecting Kv channels in other ways. Interestingly, a second PUFA site of action on Kv channels was recently identified in the ion-conducting pore (Decher et al., 2010). PUFA binding to this site induces fast channel inactivation and thereby K current inhibition. In earlier work, we have noted PUFA-induced Shaker channel inactivation induced by the application of arachidonyl amine (Börjesson et al., 2010) and high (≥210 µM) concentrations of PUFA (Börjesson et al., 2008). The Shaker channel possesses the critical isoleucine for pore block (Decher et al., 2010), suggesting that the inactivation previously reported by us may be explained by compound binding to the second site where the effect is not dependent on the charge of the compound.

Channel specificity

The critical role of the charge of residues close to PUFAs suggests that different channels may be differently sensitive to PUFAs depending on their charge profile. Channels with several positive charges at the outer half of S3 and S4 may potentially be more PUFA sensitive. For instance, Kv2.1 lacks R1 but instead possesses two arginines further extracellular at positions corresponding to 358 and 359 in Shaker, having the potential to enhance the PUFA effect. Channels like Kv4.1, Kv4.2, and Kv11.1 lacking R1 could, on the contrary, be less PUFA sensitive. In support of this prediction, the PUFA arachidonic acid does not shift the voltage dependence of neither the activation nor the steady-state inactivation

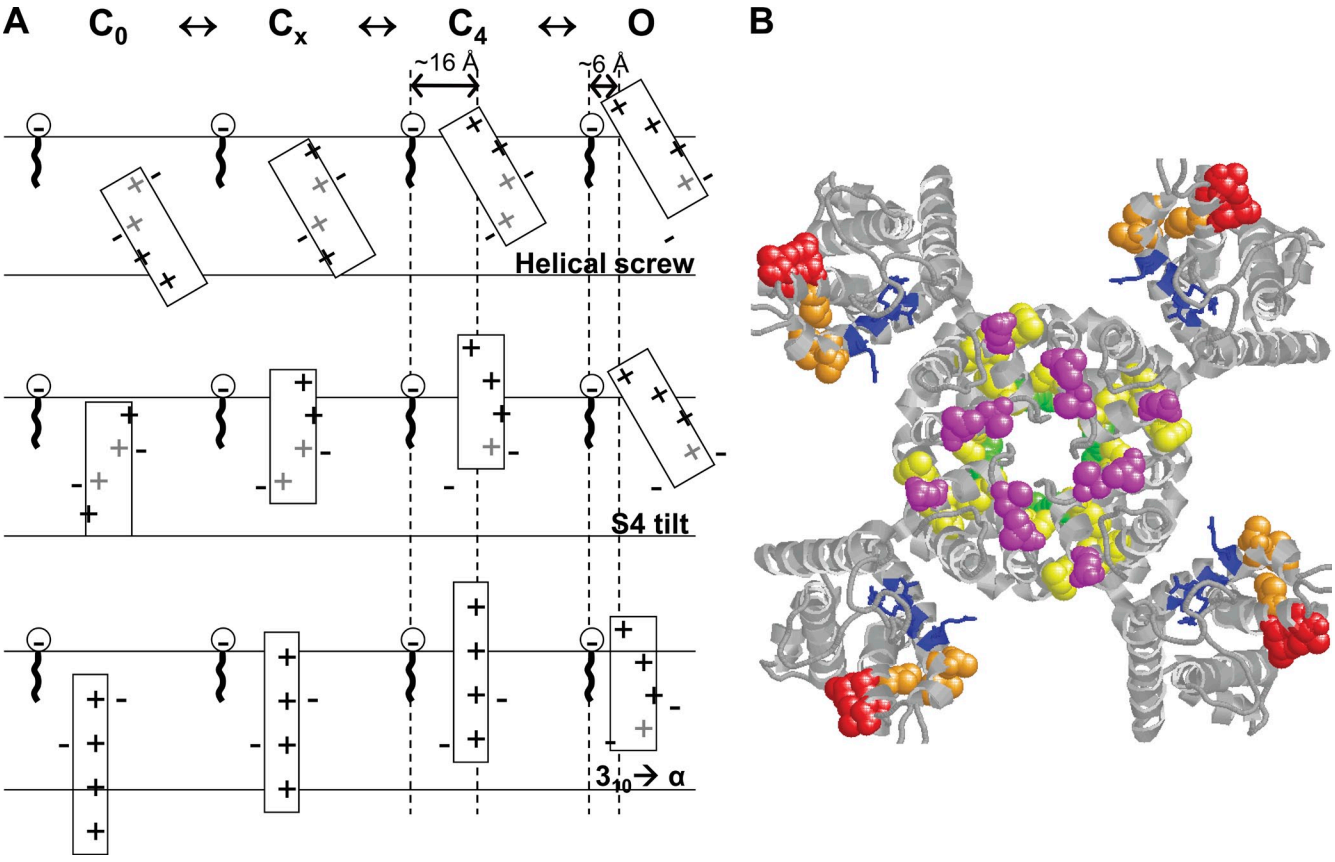

Figure 8. Possible interpretations of differential effects on different steps. (A) Three possible models for the S4 movement during the opening step. (B) The new PUFA action site compared with previously described sites. The Shaker channel is viewed from the extracellular side. The color coding follows that from Fig. 1 C. Green denote residues critical for the binding of quaternary ammonium compounds, magenta is for pore-blocking toxins, red is for voltage sensor–trapping toxins, yellow is for retigabine, and orange is for PUFA in the present investigation. The gating charges R362, R365, R368, and R371 are marked as blue sticks.

of Kv4.2 (Villarroel and Schwarz, 1996). Both the location of the PUFA site of action and the electrostatic mechanism on the opening step provide an interesting mechanistic basis for future development of small-molecule compounds to modulate electrical excitability to target epilepsy and cardiac arrhythmia.

We thank Lucas Cleve for some of the experiments; Björn Wallner and Erik Lindahl for the Kv1.2/2.1-based Shaker channel structure; Ehud Isacoff for the ILT and ILT/W434F clones; and Peter Larsson, Anders Blomqvist, and Stefan Thor for comments on the manuscript.

This work was supported by the Swedish Research Council, the Swedish Heart-Lung Foundation, the Swedish Brain Foundation, the County Council of Östergötland, Queen Silvia's Anniversary Foundation, King Gustaf V and Queen Victoria's Freemasons Foundation, Stina and Birger Johansson's Foundation, and the Swedish Society for Medical Research.

Kenton J. Swartz served as editor.

Submitted: 21 January 2011
Accepted: 22 April 2011

REFERENCES

Baker, O.S., H.P. Larsson, L.M. Mannuzzu, and E.Y. Isacoff. 1998. Three transmembrane conformations and sequence-dependent displacement of the S4 domain in shaker K+ channel gating. *Neuron.* 20:1283–1294. doi:10.1016/S0896-6273(00)80507-3

Bjelkmar, P., P.S. Niemelä, I. Vattulainen, and E. Lindahl. 2009. Conformational changes and slow dynamics through microsecond polarized atomistic molecular simulation of an integral Kv1.2 ion channel. *PLOS Comput. Biol.* 5:e1000289. doi:10.1371/journal.pcbi.1000289

Blom, S.M., N. Schmitt, and H.S. Jensen. 2009. The acrylamide (S)-2 as a positive and negative modulator of Kv7 channels expressed in Xenopus laevis oocytes. *PLoS ONE.* 4:e8251. doi:10.1371/journal.pone.0008251

Boland, L.M., and M.M. Drzewiecki. 2008. Polyunsaturated fatty acid modulation of voltage-gated ion channels. *Cell Biochem. Biophys.* 52:59–84. doi:10.1007/s12013-008-9027-2

Börjesson, S.I., and F. Elinder. 2008. Structure, function, and modification of the voltage sensor in voltage-gated ion channels. *Cell Biochem. Biophys.* 52:149–174. doi:10.1007/s12013-008-9032-5

Börjesson, S.I., S. Hammarström, and F. Elinder. 2008. Lipoelectric modification of ion channel voltage gating by polyunsaturated fatty acids. *Biophys. J.* 95:2242–2253. doi:10.1529/biophysj.108.130757

Börjesson, S.I., T. Parkkari, S. Hammarström, and F. Elinder. 2010. Electrostatic tuning of cellular excitability. *Biophys. J.* 98:396–403. doi:10.1016/j.bpj.2009.10.026

Broomand, A., and F. Elinder. 2008. Large-scale movement within the voltage-sensor paddle of a potassium channel-support for a helical-screw motion. *Neuron.* 59:770–777. doi:10.1016/j.neuron.2008.07.008

Broomand, A., R. Männikkö, H.P. Larsson, and F. Elinder. 2003. Molecular movement of the voltage sensor in a K channel. *J. Gen. Physiol.* 122:741–748. doi:10.1085/jgp.200308927

Catterall, W.A. 1986. Voltage-dependent gating of sodium channels: correlating structure and function. *Trends Neurosci.* 9:7–10. doi:10.1016/0166-2236(86)90004-4

Catterall, W.A., S. Cestèle, V. Yarov-Yarovoy, F.H. Yu, K. Konoki, and T. Scheuer. 2007. Voltage-gated ion channels and gating modifier toxins. *Toxicon.* 49:124–141. doi:10.1016/j.toxicon.2006.09.022

DeCaen, P.G., V. Yarov-Yarovoy, E.M. Sharp, T. Scheuer, and W.A. Catterall. 2009. Sequential formation of ion pairs during activation of a sodium channel voltage sensor. *Proc. Natl. Acad. Sci. USA.* 106:22498–22503. doi:10.1073/pnas.0912307106

Decher, N., A.K. Streit, M. Rapedius, M.F. Netter, S. Marzian, P. Ehling, G. Schlichthörl, T. Craan, V. Renigunta, A. Köhler, et al. 2010. RNA editing modulates the binding of drugs and highly unsaturated fatty acids to the open pore of Kv potassium channels. *EMBO J.* 29:2101–2113. doi:10.1038/emboj.2010.88

Elinder, F., and P. Århem. 2003. Metal ion effects on ion channel gating. *Q. Rev. Biophys.* 36:373–427. doi:10.1017/S0033583504003932

Elinder, F., P. Århem, and H.P. Larsson. 2001a. Localization of the extracellular end of the voltage sensor S4 in a potassium channel. *Biophys. J.* 80:1802–1809. doi:10.1016/S0006-3495(01)76150-4

Elinder, F., R. Männikkö, and H.P. Larsson. 2001b. S4 charges move close to residues in the pore domain during activation in a K channel. *J. Gen. Physiol.* 118:1–10. doi:10.1085/jgp.118.1.1

Guy, H.R., and P. Seetharamulu. 1986. Molecular model of the action potential sodium channel. *Proc. Natl. Acad. Sci. USA.* 83:508–512. doi:10.1073/pnas.83.2.508

Holmgren, M., Y. Liu, Y. Xu, and G. Yellen. 1996. On the use of thiol-modifying agents to determine channel topology. *Neuropharmacology.* 35:797–804. doi:10.1016/0028-3908(96)00129-3

Hoshi, T., W.N. Zagotta, and R.W. Aldrich. 1990. Biophysical and molecular mechanisms of Shaker potassium channel inactivation. *Science.* 250:533–538. doi:10.1126/science.2122519

Keynes, R.D., and F. Elinder. 1998a. Modelling the activation, opening, inactivation and reopening of the voltage-gated sodium channel. *Proc. Biol. Sci.* 265:263–270. doi:10.1098/rspb.1998.0291

Keynes, R.D., and F. Elinder. 1998b. On the slowly rising phase of the sodium gating current in the squid giant axon. *Proc. Biol. Sci.* 265:255–262. doi:10.1098/rspb.1998.0290

Keynes, R.D., and F. Elinder. 1999. The screw-helical voltage gating of ion channels. *Proc. Biol. Sci.* 266:843–852. doi:10.1098/rspb.1999.0714

Kopljar, I., A.J. Labro, E. Cuypers, H.W. Johnson, J.D. Rainier, J. Tytgat, and D.J. Snyders. 2009. A polyether biotoxin binding site on the lipid-exposed face of the pore domain of Kv channels revealed by the marine toxin gambierol. *Proc. Natl. Acad. Sci. USA.* 106:9896–9901. doi:10.1073/pnas.0812471106

Lainé, M., M.C. Lin, J.P. Bannister, W.R. Silverman, A.F. Mock, B. Roux, and D.M. Papazian. 2003. Atomic proximity between S4 segment and pore domain in Shaker potassium channels. *Neuron.* 39:467–481. doi:10.1016/S0896-6273(03)00468-9

Lange, W., J. Geissendörfer, A. Schenzer, J. Grötzinger, G. Seebohm, T. Friedrich, and M. Schwake. 2009. Refinement of the binding site and mode of action of the anticonvulsant Retigabine on KCNQ K+ channels. *Mol. Pharmacol.* 75:272–280. doi:10.1124/mol.108.052282

Leaf, A., Y.F. Xiao, J.X. Kang, and G.E. Billman. 2003. Prevention of sudden cardiac death by n-3 polyunsaturated fatty acids. *Pharmacol. Ther.* 98:355–377. doi:10.1016/S0163-7258(03)00039-1

Lecar, H., H.P. Larsson, and M. Grabe. 2003. Electrostatic model of S4 motion in voltage-gated ion channels. *Biophys. J.* 85:2854–2864. doi:10.1016/S0006-3495(03)74708-0

Ledwell, J.L., and R.W. Aldrich. 1999. Mutations in the S4 region isolate the final voltage-dependent cooperative step in potassium channel activation. *J. Gen. Physiol.* 113:389–414. doi:10.1085/jgp.113.3.389

Lefevre, F., and N. Aronson. 2000. Ketogenic diet for the treatment of refractory epilepsy in children: a systematic review of efficacy. *Pediatrics.* 105:E46. doi:10.1542/peds.105.4.e46

Long, S.B., X. Tao, E.B. Campbell, and R. MacKinnon. 2007. Atomic structure of a voltage-dependent K+ channel in a lipid membrane-like environment. *Nature.* 450:376–382. doi:10.1038/nature06265

MacKinnon, R., L. Heginbotham, and T. Abramson. 1990. Mapping the receptor site for charybdotoxin, a pore-blocking potassium channel inhibitor. *Neuron.* 5:767–771. doi:10.1016/0896-6273(90)90335-D

McLaughlin, S. 1989. The electrostatic properties of membranes. *Annu. Rev. Biophys. Biophys. Chem.* 18:113–136. doi:10.1146/annurev.bb.18.060189.000553

Milescu, M., F. Bosmans, S. Lee, A.A. Alabi, J.I. Kim, and K.J. Swartz. 2009. Interactions between lipids and voltage sensor paddles detected with tarantula toxins. *Nat. Struct. Mol. Biol.* 16:1080–1085. doi:10.1038/nsmb.1679

Pathak, M., L. Kurtz, F. Tombola, and E. Isacoff. 2005. The cooperative voltage sensor motion that gates a potassium channel. *J. Gen. Physiol.* 125:57–69. doi:10.1085/jgp.200409197

Peretz, A., L. Pell, Y. Gofman, Y. Haitin, L. Shamgar, E. Patrich, P. Kornilov, O. Gourgy-Hacohen, N. Ben-Tal, and B. Attali. 2010. Targeting the voltage sensor of Kv7.2 voltage-gated K+ channels with a new gating-modifier. *Proc. Natl. Acad. Sci. USA.* 107:15637–15642. doi:10.1073/pnas.0911294107

Perozo, E., R. MacKinnon, F. Bezanilla, and E. Stefani. 1993. Gating currents from a nonconducting mutant reveal open-closed conformations in Shaker K+ channels. *Neuron.* 11:353–358. doi:10.1016/0896-6273(93)90190-3

Phillips, L.R., and K.J. Swartz. 2010. Position and motions of the S4 helix during opening of the Shaker potassium channel. *J. Gen. Physiol.* 136:629–644. doi:10.1085/jgp.201010517

Rooney, E.K., J.M. East, O.T. Jones, J. McWhirter, A.C. Simmonds, and A.G. Lee. 1983. Interaction of fatty acids with lipid bilayers. *Biochim. Biophys. Acta.* 728:159–170. doi:10.1016/0005-2736(83)90467-4

Schmidt, D., Q.X. Jiang, and R. MacKinnon. 2006. Phospholipids and the origin of cationic gating charges in voltage sensors. *Nature.* 444:775–779. doi:10.1038/nature05416

Schoppa, N.E., and F.J. Sigworth. 1998. Activation of Shaker potassium channels. III. An activation gating model for wild-type and V2 mutant channels. *J. Gen. Physiol.* 111:313–342. doi:10.1085/jgp.111.2.313

Schoppa, N.E., K. McCormack, M.A. Tanouye, and F.J. Sigworth. 1992. The size of gating charge in wild-type and mutant Shaker potassium channels. *Science.* 255:1712–1715. doi:10.1126/science.1553560

Schow, E.V., J.A. Freites, K. Gogna, S.H. White, and D.J. Tobias. 2010. Down-state model of the voltage-sensing domain of a potassium channel. *Biophys. J.* 98:2857–2866. doi:10.1016/j.bpj.2010.03.031

Sfondouris, J., L. Rajagopalan, F.A. Pereira, and W.E. Brownell. 2008. Membrane composition modulates prestin-associated charge movement. *J. Biol. Chem.* 283:22473–22481. doi:10.1074/jbc.M803722200

Shafrir, Y., S.R. Durell, and H.R. Guy. 2008. Models of voltage-dependent conformational changes in NaChBac channels. *Biophys. J.* 95:3663–3676. doi:10.1529/biophysj.108.135335

Sigg, D., E. Stefani, and F. Bezanilla. 1994. Gating current noise produced by elementary transitions in Shaker potassium channels. *Science.* 264:578–582. doi:10.1126/science.8160016

Smith-Maxwell, C.J., J.L. Ledwell, and R.W. Aldrich. 1998. Uncharged S4 residues and cooperativity in voltage-dependent potassium channel activation. *J. Gen. Physiol.* 111:421–439. doi:10.1085/jgp.111.3.421

Swartz, K.J. 2007. Tarantula toxins interacting with voltage sensors in potassium channels. *Toxicon.* 49:213–230. doi:10.1016/j.toxicon.2006.09.024

Swartz, K.J., and R. MacKinnon. 1997. Mapping the receptor site for hanatoxin, a gating modifier of voltage-dependent K+ channels. *Neuron.* 18:675–682. doi:10.1016/S0896-6273(00)80307-4

Tao, X., A. Lee, W. Limapichat, D.A. Dougherty, and R. MacKinnon. 2010. A gating charge transfer center in voltage sensors. *Science.* 328:67–73. doi:10.1126/science.1185954

Tiwari-Woodruff, S.K., M.A. Lin, C.T. Schulteis, and D.M. Papazian. 2000. Voltage-dependent structural interactions in the Shaker K^+ channel. *J. Gen. Physiol.* 115:123–138. doi:10.1085/jgp.115.2.123

Tombola, F., M.M. Pathak, and E.Y. Isacoff. 2006. How does voltage open an ion channel? *Annu. Rev. Cell Dev. Biol.* 22:23–52. doi:10.1146/annurev.cellbio.21.020404.145837

Villarroel, A., and T.L. Schwarz. 1996. Inhibition of the Kv4 (Shal) family of transient K+ currents by arachidonic acid. *J. Neurosci.* 16:1016–1025.

Xiong, Q., H. Sun, and M. Li. 2007. Zinc pyrithione-mediated activation of voltage-gated KCNQ potassium channels rescues epileptogenic mutants. *Nat. Chem. Biol.* 3:287–296. doi:10.1038/nchembio874

Xu, X.P., D. Erichsen, S.I. Börjesson, M. Dahlin, P. Åmark, and F. Elinder. 2008. Polyunsaturated fatty acids and cerebrospinal fluid from children on the ketogenic diet open a voltage-gated K channel: a putative mechanism of antiseizure action. *Epilepsy Res.* 80:57–66. doi:10.1016/j.eplepsyres.2008.03.013

Xu, Y., Y. Ramu, and Z. Lu. 2008. Removal of phospho-head groups of membrane lipids immobilizes voltage sensors of K+ channels. *Nature.* 451:826–829. doi:10.1038/nature06618

Zagotta, W.N., T. Hoshi, and R.W. Aldrich. 1994. Shaker potassium channel gating. III: evaluation of kinetic models for activation. *J. Gen. Physiol.* 103:321–362. doi:10.1085/jgp.103.2.321

Zhou, M., J.H. Morais-Cabral, S. Mann, and R. MacKinnon. 2001. Potassium channel receptor site for the inactivation gate and quaternary amine inhibitors. *Nature.* 411:657–661. doi:10.1038/35079500